Influence of Frequency Offset on Modified EGC Diversity Receiver

Bojana Z. Nikolić, *Student Member, IEEE,* Bojan R. Dimitrijević, *Member, IEEE,* Nenad D. Milošević, *Member, IEEE,* and Goran T. Đorđević, *Member, IEEE*

***Abstract* — In this paper a performance analysis of a modified M-ary phase-shift-keying (MPSK) signal diversity receiver with a predetection equal gain combiner (EGC) will be presented. The modification is in introducing a structure that performs the estimation with remodulation (ER). The EGC combining is realized by using a constant modulus algorithm (CMA). The influence of carrier frequency offset, length of ER structure and other parameters of the receiver will be examined.**

***Keywords* — Constant modulus algorithm, diversity, estimation with remodulation, frequency offset, phase-locked loop.**

I. Introduction

In wireless communication systems the variation of instantaneous value of the received signal, i.e. fading of the signal envelope is one of the main causes of performance degradation in wireless communication systems [1]. Various diversity combining techniques [1] are used to combat the deleterious effect of channel fading without enlarging either transmitting power or bandwidth of the channel. In equal-gain combining (EGC), the received signals from all branches are co-phased in order to eliminate the random signal phase fluctuations occurring during transmission, equally weighted and then summed to form a decision variable. Since the EGC technique achieves performances comparable to the ones of the maximum ratio combining (MRC) technique, but with lower implementation complexity, this technique has received great interest in the literature [2]–[4].

In practice, EGC is often realized using a constant modulus algorithm (CMA). Constant modulus (CM) based algorithms have been widely used for blind beamforming, multiuser detection and equalization [5]–[8].

In [9] a modification of the EGC diversity receiver of quadrature phase shift keying (QPSK) signal, using CMA for cophasing and phase-locked loop (PLL) for carrier synchronization is proposed. The modification is related to the introduction of a structure that performs the estimation with remodulation (ER). With an adequate choice of the parameters for ER+PLL block the proposed receiver can operate within a wider carrier frequency offset range with a very small variation of the performance in comparison with the receiver using only PLL.

In this paper a performance analysis of a modified M-ary phase-shift-keying (MPSK) signal diversity receiver with predetection EGC will be presented. The modification is in introducing a structure that performs the estimation with remodulation. The EGC combining is realized by using CMA. The influence of carrier frequency offset, length of ER structure and other parameters of the receiver will be examined.

II. System Model

A block diagram of the proposed EGC receiver with a PLL detector is shown on the example of QPSK signal detection in Fig. 1. The basic idea is to process the signal after the EGC in such a way that the noise variance is lowered and the useful signal is damaged as little as possible [9]. In that case the PLL bandwidth may be higher, which provides a lower sensitivity to the frequency offset. The introduced ER structure fulfils the aforementioned requirement and it is placed between EGC and PLL. In the proposed diversity receiver ER structure and PLL make a block which will be referred to as ER+PLL. If the ER structure is omitted, we get an ordinary EGC diversity receiver [1].

Let the signal at the output of each of the receiving N_a antennas be

$$r_n(t) = s_n(t) + z_n(t), \; n = 0,1,..., N_a - 1, \tag{1}$$

where $z_n(t)$ is the white Gaussian noise, and $s_n(t)$ is the MPSK signal with a rectangular symbol pulse shape

$$s_n(t) = e^{j\hat{\theta}(t-\tau_n)} \exp\big(j(\omega_c + \Delta\omega)(t - \tau_n)\big), \tag{2}$$

with

$$\hat{\theta}(t) = \frac{2\pi}{M}\hat{d}(t), \tag{3}$$

where τ_n is the delay at n-th path and M is the number of modulation levels. Symbol $\hat{d}(t)$ can take one of the following values

$$\begin{aligned} &\hat{d}(t) \in \{0,\ldots, M-1\}, \\ &kT_s \le t < (k+1)T_s, \; k = 0,1,2,... \end{aligned} \tag{4}$$

The symbol interval is T_s, ω_c is the locally generated fixed reference carrier frequency and $\Delta\omega$ is the frequency offset.

This work is supported in part by the Ministry of Education, Science and Technological Development of Serbia within the Project TR-32051.

Corresponding author Bojana Z. Nikolić is with the Faculty of Electronic Engineering, University of Niš, A. Medvedeva 14, 18 000 Niš, Serbia (phone: 381-18-529423; e-mail: bojana.nikolic@elfak.ni.ac.rs).

Bojan R. Dimitrijević is with the Faculty of Electronic Engineering, University of Niš, A. Medvedeva 14, 18 000 Niš, Serbia (phone: 381-18-529367; e-mail: bojan.dimitrijevic@elfak.ni.ac.rs).

Nenad D. Milošević is with the Faculty of Electronic Engineering, University of Niš, A. Medvedeva 14, 18 000 Niš, Serbia (phone: 381-18-529367; e-mail: nenad.milosevic@elfak.ni.ac.rs).

Goran T. Đorđević is with the Faculty of Electronic Engineering, University of Niš, A. Medvedeva 14, 18 000 Niš, Serbia (phone: 381-18-529304; e-mail: goran@elfak.ni.ac.rs).

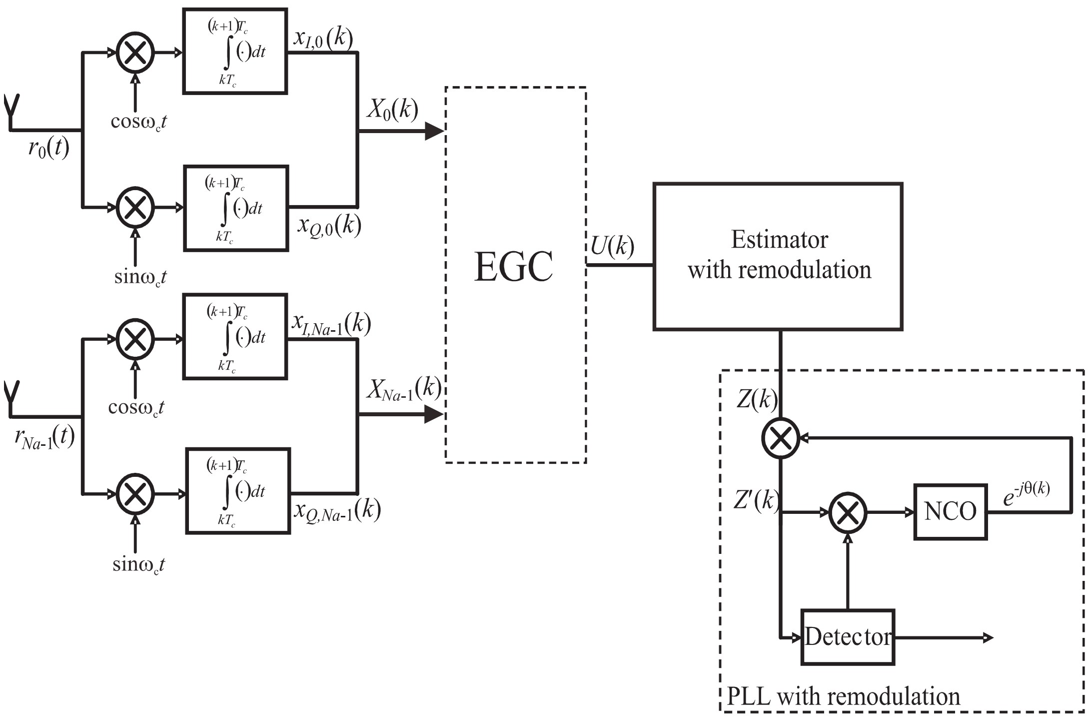

Fig. 1. Block diagram of the receiver.

After multiplication by the fixed frequency reference carrier and passing through the integrate and dump circuit, the complex baseband signal at the input of the EGC block can be expressed as

$$X_n(k) = \int_{kT_s}^{(k+1)T_s} r_n(t)\cos(\omega_c t)dt + j \int_{kT_s}^{(k+1)T_s} r_n(t)\sin(\omega_c t)dt\,, \quad (5)$$

where k denotes the discrete time corresponding to the output of the integrate and dump circuit.

In EG combiner, a co-phasing of the input branches is performed using CMA, and the output signal can be expressed as

$$U(k) = \sum_{n=0}^{N_a-1} X_n(k)V_n(k)\,, \quad (6)$$

where N_a is the number of diversity branches. $V_n(k)$ is the weight of the n-th branch obtained by the CMA and may be written as [10]

$$V_n(k) = \\ = V_n(k-1) + \mu_V\left(\frac{1}{|U(k-1)|} - 1\right)U(k-1)X_n^*(k-1) ,\quad (7)$$

where μ_V is the adaptation factor, and $(\cdot)^*$ denotes the complex conjugate.

The signal $U(k)$, is next lead to the ER structure, which is an estimator with remodulation, and its operation is described by the following equations

$$Z(k) = \sum_{l=-L}^{L} Y(k-l)R_l(k)W_l(k)\,, \quad (8)$$

where $2L$ is the ER structure length, and $Y(k+L) = U(k)$. The weights $W_l(k)$ are being adjusted by the Leaky LMS algorithm [11]

$$\begin{aligned} &W_0(k) = 1, \\ &W_l(k+1) = \\ &= (1-\mu_W)W_l(k) + \mu_W Y(k)\cdot(Y(k-l)\cdot R_l(k))^*, \\ &l = -L,...,L, \quad l \neq 0, \end{aligned} \quad (9)$$

where μ_W is the adaptation factor, and $R_l(k)$ are remodulation weights, which are determined as

$$\begin{aligned} &R_0(k) = 1, \\ &R_l(k) = \exp\left(j\frac{2\pi}{M} \times \right. \\ &\left. \times \underset{p\in\{0,\ldots,M-1\}}{\arg\min} \left\{ e^{j\frac{2\pi}{M}p} Y^*(k-l)W_l^*(k)Y(k) \right\} \right), \\ &l = -L,...,L, \quad l \neq 0. \end{aligned} \quad (10)$$

Carrier synchronization is performed by the second order remodualtion PLL [12]. In a digital domain, a remodulation PLL consists of a remodulation circuit and a numerically controlled oscillator (NCO). Phase difference in the NCO is equal to the argument of the remodulated signal

$$\Delta\varphi(k) = \arg\left\{ Z(k)\cdot e^{-j\theta(k)} \cdot \exp\left(-j\frac{2\pi}{M}d(k)\right)\right\}, \quad (11)$$

with $\theta(k)$ being the phase of the signal at the output of NCO for the k-th sampling interval. This parameter will be defined later.

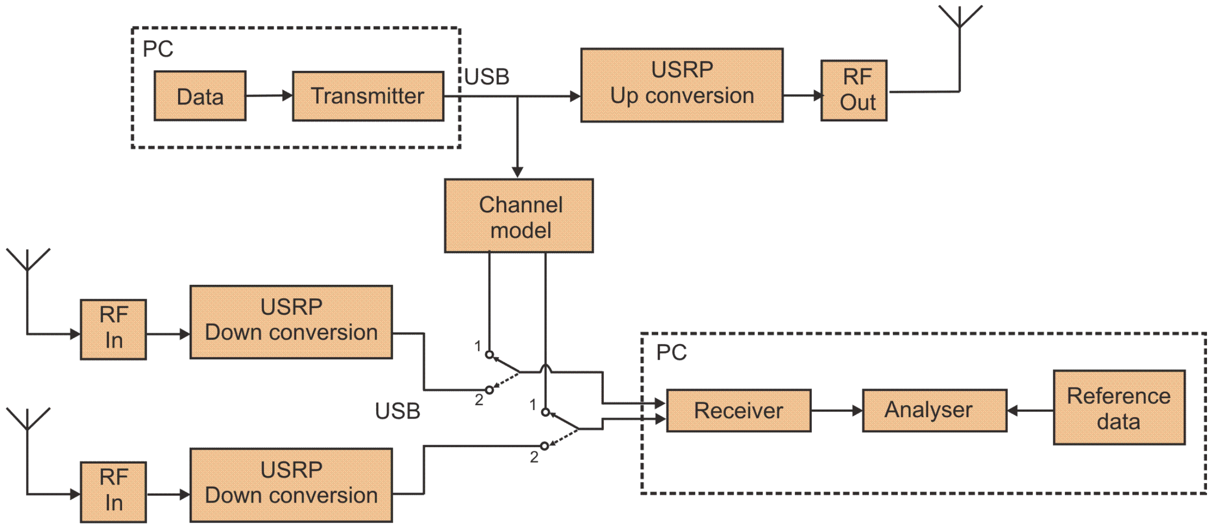

Fig. 2. Block diagram of the simulation and experimental setup.

The phase difference is filtered within the NCO using a first order low pass filter

$$e(k) = (1 - A_{PLL})e(k-1) + A_{PLL} \cdot \Delta\varphi(k-1), \quad (12)$$

where $e(k)$ is the filter output, and A_{PLL} is the filter constant that can take values from (0,1].

The NCO frequency correction is obtained by

$$\delta f(k) = \frac{1}{2\pi} \frac{K_{PLL}}{T_S} e(k), \quad (13)$$

where K_{PLL} is the normalized gain used for the adjustment of the frequency correction value.

The phase $\theta(k)$ is obtained by the integration of frequency correction values

$$\theta(k) = \theta(0) + \frac{2\pi}{T_S} \sum_{m=1}^{k} \delta f(m). \quad (14)$$

The decision is made using the following minimization

$$d(k) = \underset{p \in \{0,\ldots,M-1\}}{\arg\min} \left\{ \exp\left(j \frac{2\pi}{M} p \right) Z'^{*}(k) \right\}. \quad (15)$$

The performance of the algorithm described in this section is determined by the Monte-Carlo simulation on the computer.

III. Simulation

The functionality and properties of the diversity receiver, considered in this paper, are verified through both a simulation and an experiment on a system based on universal software radio peripheral (USRP) hardware. However, since the simulation offers a wider range of possibilities, concerning conditions in propagation environment and the characteristics of the receiver, all the results, presented here, are obtained by the simulation.

The block diagram of simulation and experimental setup is shown in Fig. 2. The simulation setup contains a complete software simulation chain in PC, including a transmitter, channel, and receiver. In the experiment, the baseband processing is performed in PC, up/down conversion is performed in USRP hardware, and the communication channel is real.

Blocks marked with PC are common to both simulation and experimental setup. They run on Linux and are written in C++. The same pseudorandom sequence is generated and repeated within *Data* and *Reference data* blocks, so that the transmitted and the received data can be compared. A *transmitter* block performs baseband processing and generates a QPSK modulated signal. Depending on whether the simulation or the experiment is performed, a QPSK signal is next led to the simulated channel or to the USRP via a USB interface. The communication at the USB interface is performed using *libusb* library. USRP receives data from the USB interface and performs digital to analog conversion and up-conversion to 2.4 GHz band. At the receiver chain, similar processing is performed. In the case of the experiment, after down-conversion and analog to digital conversion in USRP, signal is transferred via the USB interface to PC. In case the simulation is performed, signal from the *Channel model* block is led directly to the receiver. A *Receiver* block performs demodulation and baseband processing. The received data are compared to the sent data in an *Analyzer* block.

IV. Simulation Results

In the following figures the performance of the modified EGC receiver (referred to as ER+PLL) is compared with the one of the ordinary EGC diversity receiver (referred to as PLL) when a MPSK signal is detected. Two values of loop parameter K_{PLL} are chosen to be considered: value K_{PLL}=0.2 that supports the operating mode of the ordinary PLL receiver and K_{PLL}=1, which is an optimal value for the operation of the modified ER+PLL receiver.

In Fig.3, Fig. 4 and Fig. 5 the influence of the ER filter length on performance of BPSK, QPSK and 8PSK signal receiver is presented, respectively. Two cases are considered: with and without a frequency offset. When the BPSK signal detection is considered (Fig. 3), all characteristics are the same, regardless of the operating mode of PLL or the presence of constant frequency offset. In cases of QPSK and 8PSK signal detection (Fig. 4 and Fig. 5), in the absence of frequency offset it can be noticed that the receiver shows a better performance for K_{PLL}=0.2 and the presence of ER filter of a higher order in that case doesn't impair the performance significantly. However, when there is a frequency offset the performance either gets impaired (QPSK case) or the receiver totally loses the synchronization (8PSK case) for K_{PLL}=0.2. On the other hand, in the same conditions the performance remains very good when K_{PLL}=1 holds.

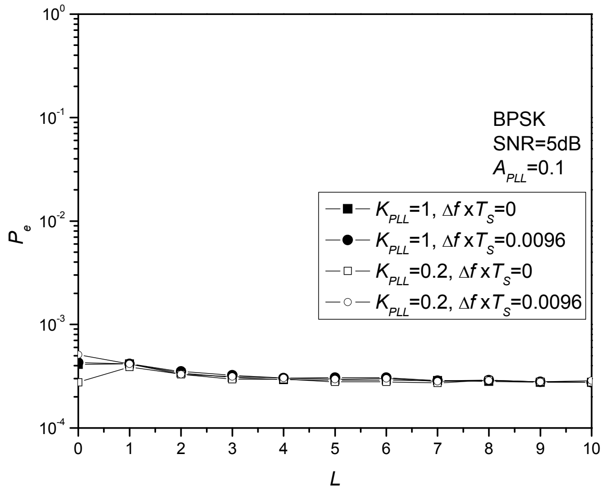

Fig. 3. Error probability as a function of ER filter length for the case of BPSK signal detection.

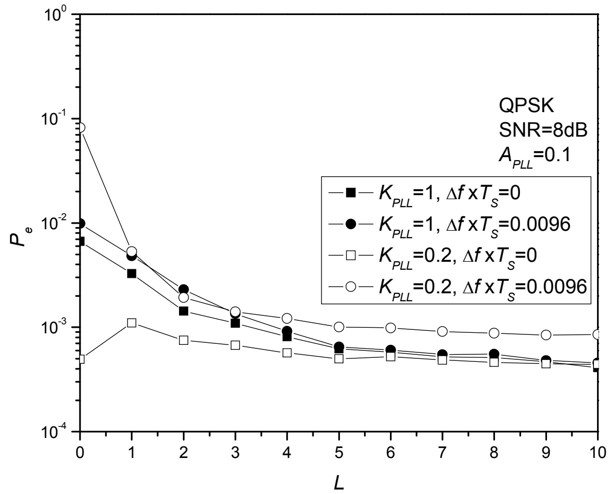

Fig. 4. Error probability as a function of ER filter length for the case of QPSK signal detection.

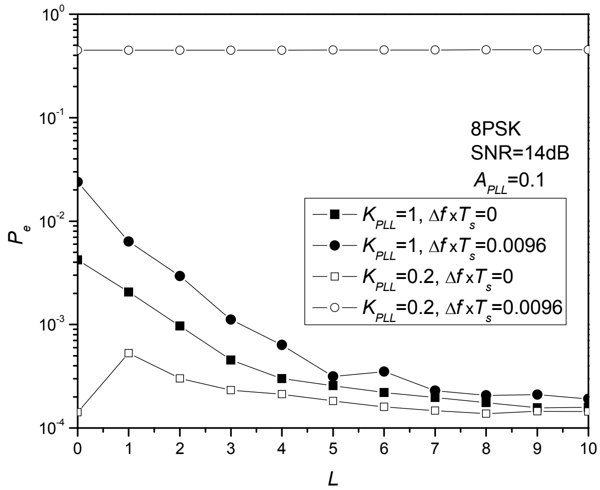

Fig. 5. Error probability as a function of ER filter length for the case of 8PSK signal detection.

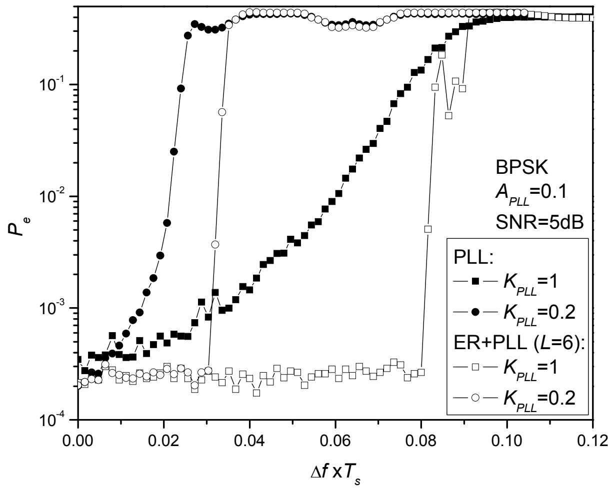

Fig. 6. Error probability as a function of carrier frequency offset for BPSK signal detection.

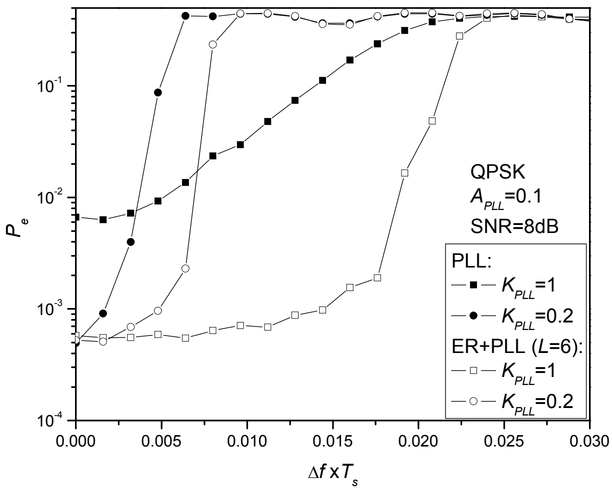

Fig. 7. Error probability as a function of carrier frequency offset for QPSK signal detection.

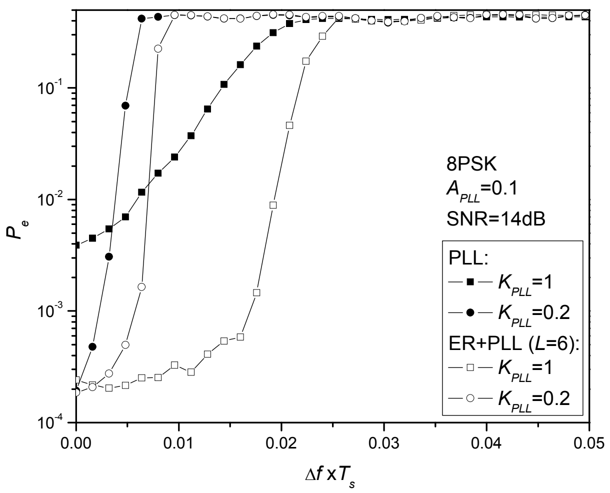

Fig. 8. Error probability as a function of carrier frequency offset for 8PSK signal detection.

In Fig. 6, Fig. 7 and Fig. 8 the dependence of BER on the normalized frequency offset can be traced for BPSK, QPSK and 8PSK signal detection, respectively. Similar behavior and tendencies can be noticed in all three cases. Regardless of the K_{PLL} value, the frequency offset, which allows PLL to stay in synchronism, is much larger when the ER block is included. At the same time performances either stay approximately the same or get improved. This clearly shows that the use of modified EGC receiver of PSK signal brings the expected performance gain for all considered numbers of modulation levels.

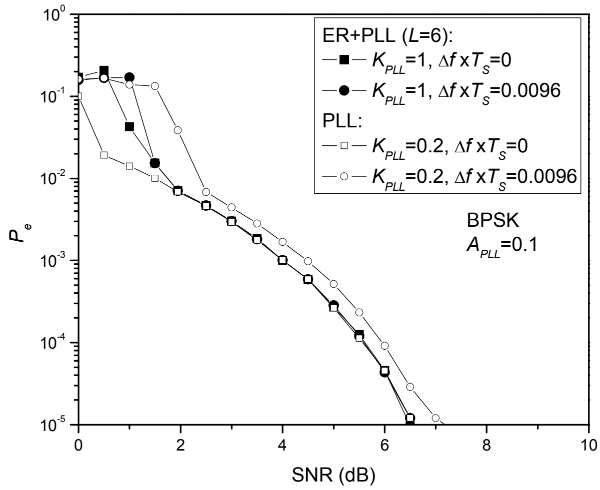

Fig. 9. Error probability as a function of signal to noise ratio for BPSK signal detection.

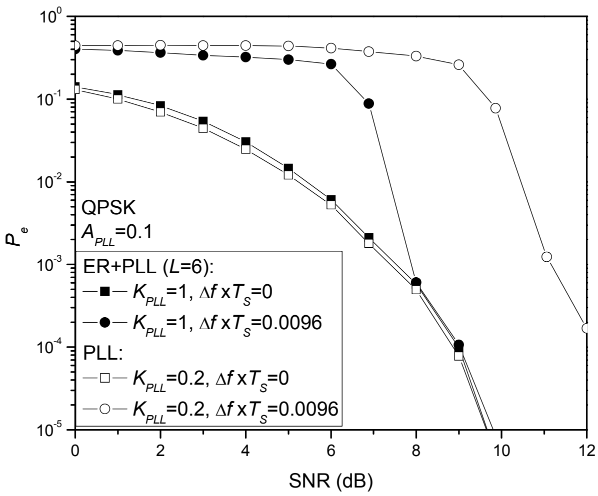

Fig. 10. Error probability as a function of signal to noise ratio for QPSK signal detection

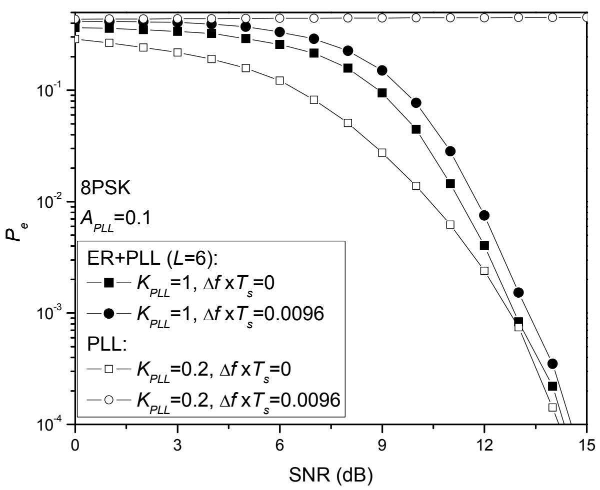

Fig. 11. Error probability as a function of signal to noise ratio for 8PSK signal detection.

In Fig.9, Fig.10 and Fig.11 the BER as a function of average input SNR is presented for BPSK, QPSK and 8PSK signal detection, respectively. As one can see, the behavior and tendencies that are being noticed and analyzed in previous figures (Fig. 6, Fig. 7 and Fig. 8) at one fixed SNR value refer also to the wide range of average input SNR.

V. Conclusion

In this paper a performance analysis of a modified MPSK signal diversity receiver with predetection EGC is presented.

For all considered numbers of modulation levels in PSK signal detection, the use of a modified EGC receiver allows a significantly larger frequency offset than the diversity receiver using only a PLL. At the same time performances either stay approximately the same or get improved.

The behavior and tendencies that are being noticed at one fixed value refer also to the wide range of average input SNR.

References

[1] M. K. Simon and M. S. Alouini, *Digital communication over fading channels: A unified approach to performance analysis*. New York: Wiley, 2000.

[2] A. Annamalai, C. Tellambura, and V. K. Bhargava, “Equal-gain diversity receiver performance in wireless channels,” *IEEE Transactions on Communications*, vol. 48, no. 10, pp. 1732-1745, October 2000.

[3] M. A. Najib and V. K. Prabhu, “Analysis of equal-gain diversity with partially coherent fading signals,” *IEEE Transactions on Vehicular Technology*, vol. 49, no. 3, pp.783-791, May 2000.

[4] N. C. Sagias and G. K. Karagiannidis, “Effects of carrier phase error on EGC receivers in correlated Nakagami-m fading,” *IEEE Communications Letters*, vol. 9, no. 7, pp.580-582, July 2005.

[5] R. Gooch and J. Lundell, “CM array: an adaptive beamformer for constant modulus signals,” in *Proc. IEEE International Conference on Acoustics, Speech, and Signal Processing*, Tokyo, 1986, pp. 2523–2526.

[6] L. C. Godara, “Application of antenna arrays to mobile communications, Part II: Beam-forming and direction-of-arrival estimation,” *Proceedings of the IEEE*, vol. 85, pp. 1195–1245, August 1997.

[7] C. R. Johnson, P. Schniter, T. J. Endres, J. D. Behm, D. R. Brown, and R. A. Casas, “Blind equalization using the constant modulus criterion: A review,” *Proceedings of the IEEE*, vol. 86, no. 10, pp. 1927–1950, October 1998.

[8] S. Chen, A. Wolfgang, and L. Hanzo, “Constant modulus algorithm aided soft decision directed scheme for blind space-time equalisation of simo channels,” *Signal Processing*, vol. 87, pp. 2587–2599, November 2007.

[9] B. Nikolić, B. Dimitrijević, N. Milošević and G. T. Đorđević, "Performance improvement of QPSK signal predetection EGC diversity receiver", *Radioengineering*, vol. 21, no. 3, pp. 831-837, September 2012.

[10] D. Godard, "Self-recovering equalization and carrier tracking in two-dimensional data communication systems", *IEEE Transactions on Communications*, vol. 28, no. 11, pp. 1867-1875, November 1980.

[11] W. Sethares, D. Lawrence, C. J. R. Johnson and R. Bitmead, "Parameter drift in LMS adaptive filters", *IEEE Transactions on Acoustics, Speech and Signal Processing*, vol. 34, no. 4, pp. 868-879, August 1986.

[12] F. M. Gardner, *Phase lock techniques*. New York: Wiley, 1979.